Electronic Supplementary Material (ESI) for ChemComm.

Supporting Materials

Effect of Ligand Structures on the Size Control of Mono- and Bi-Thiolate-Protected Silver Nanoclusters

Kaiyuan Zheng,[a] Xun Yuan,[b,]* and Jianping Xie[a,]*

[a] Department of Chemical and Biomolecular Engineering, National University of Singapore, 4 Engineering Drive 4, 117585, Singapore

[b] College of Materials Science and Engineering, Qingdao University of Science and Technology, Qingdao 266042, P. R. China

CORRESPONDING AUTHOR FOOTNOTE. * To whom the correspondence should be addressed.

E-mail: chexiej@nus.edu.sg (Prof. J. Xie) and yuan916xun@gmail.com (Dr. X. Yuan)

Tel: +65 6516 1067 (Prof. J. Xie) and +65 97640196 (Dr. X. Yuan)

EXPERIMENTAL SECTION

1. Materials

Ultrapure water (18.2 MΩ) was used throughout the study. All glassware and magnetic stir bars were washed with diluted nitric acid and *aqua regia*, rinsed with abundant ethanol and water, and dried in an oven before use. All chemicals were commercially available and used as received: 3-mercaptopropionic acid (MPA), 4-mercaptobutyric acid (MTBA), 6-mercaptohexanoic acid (MHA), sodium borohydride ($NaBH_4$), *para*-mercaptobenzoic acid (*p*-MBA), and glutathione (GSH) were purchased from Sigma-Aldrich; silver nitrate ($AgNO_3$) and sodium hydroxide (NaOH) were purchased from Merck; ethanol was purchased from Fisher.

2. Instruments

UV-vis absorption spectra were recorded by a Shimadzu UV-1800 spectrometer. Native polyacrylamide gel electrophoresis (PAGE) was carried out on a Bio-Rad Mini-Protean Tetra Cell system using discontinuous gels (1.0 × 83 × 73 mm). 20 wt% and 4 wt% acrylamide monomers were prepared for resolving and stacking gels, respectively. Electrospray ionization mass spectra (ESI-MS) of Ag nanoclusters (NCs) were acquired on a Bruker microTOF-Q system.

3. Synthesis of alkane-thiol-protected Ag_{25} NCs

Aqueous solutions of $AgNO_3$ (20 mM) and alkane-thiol ligands (10 mM) were freshly prepared with ultrapure water. In a typical synthesis of $Ag_{25}(MHA)_{18}$ NCs, aqueous solutions of $AgNO_3$ (20 mM, 0.125 mL; as silver precursor) and MHA (10 mM, 0.5 mL; as protecting ligand) were mixed in water (4.225 mL) or mixed solvents of ethanol/water (up to 40 vol% of ethanol) to form Ag(I)-MHA complexes with an opalescent color under stirring condition at 50 °C. Next, NaOH solution (1 M) was added to the system to adjust the pH to ~11-12. Afterwards, fresh $NaBH_4$ solution (0.1 mL, prepared by dissolving 43 mg of $NaBH_4$ powder in 10 mL of 0.2 M NaOH solution) was added dropwise to reduce the complexes. The $Ag_{25}(MHA)_{18}$ NCs were collected after 30 min for further characterization. By using the same synthetic conditions, MTBA- and MPA-protected Ag_{25} NCs can also be synthesized.

4. Synthesis of *p*-MBA-protected Ag_{44} NCs

In a typical synthesis of Ag_{44}(*p*-MBA)$_{30}$ NCs, an aqueous solution of $AgNO_3$ (20 mM, 0.125 mL; as silver precursor) and an ethanolic solution of *p*-MBA (50 mM, 0.1 mL; as protecting ligand) were added to a mixed solvent of ethanol/water (4.625 mL, from 0 vol% to 40 vol% of ethanol) to form light-yellow Ag(I)-*p*-MBA complexes under stirring condition at 50 °C. Next, NaOH solution (1 M) was added to the system to adjust the pH to 12. Afterwards, fresh $NaBH_4$ solution (0.1 mL) was added dropwise to reduce the complexes. The Ag_{44}(*p*-MBA)$_{30}$ NCs were collected after 2 h.

5. Synthesis of GSH-protected $Ag_{9–15}$ NCs

In a typical synthesis, freshly prepared aqueous solutions of $AgNO_3$ (20 mM, 0.125 mL; as silver precursor) and GSH (10 mM, 0.5 mL; as protecting ligand) were mixed in water (4.225 mL) to form opalescent Ag(I)-GSH complexes under stirring condition at 50 °C. Next, NaOH solution (1 M) was added to the system to adjust the pH to ~11-12. Afterwards, fresh $NaBH_4$ solution (0.1 mL) was added dropwise to reduce the complexes. The $Ag_{9–15}(GSH)_{5\text{-}10}$ NCs were collected after 30 min.

6. Synthesis of bi-ligand-protected Ag NCs

6.1. Synthesis of bi-thiolate MHA_MPA- and MHA_GSH-protected Ag_{25} NCs

The bi-thiolate MHA_MPA- and MHA_GSH-protected Ag_{25} NCs were synthesized by using the same synthetic condition for $Ag_{25}(MHA)_{18}$ NCs except for the introduction of bi-thiolate ligands into the reaction system. Typically, aqueous solutions of MHA and MPA or GSH (10 mM) with different feeding ratios such as 4 : 1 (0.4 mL MHA and 0.1 mL MPA or GSH), or 2 : 1 (0.333 mL MHA and 0.167 mL MPA or GSH), or 1 : 1 (0.25 mL MHA and 0.25 mL MPA or GSH) were mixed with $AgNO_3$ (20 mM, 0.125 mL) in water (4.225 mL) to form Ag(I)-MHA_MPA or Ag(I)-MHA_GSH complexes, Next, NaOH solution (1 M) was added to the system to adjust the pH to ~11-12. Afterwards, fresh $NaBH_4$ solution (0.1 mL) was added dropwise to reduce the complexes. The bi-thiolate MHA_MPA- or MHA_GSH-protected Ag_{25} NCs were collected after 30 min for further characterization.

6.2. Synthesis of bi-thiolate MHA_*p*-MBA-protected Ag_{25} NCs

In a typical synthesis of bi-thiolate MHA_*p*-MBA-protected Ag NCs, an aqueous solution of MHA (50 mM) and an ethanolic solution of *p*-MBA (50 mM) with different feeding ratios such as 4 : 1 (0.08 mL MHA and 0.02 mL *p*-MBA), or 2 : 1 (0.067 mL MHA and 0.033 mL *p*-MBA), or 1 : 1 (0.05 mL MHA and 0.05 mL *p*-MBA) were mixed with $AgNO_3$ solution (20 mM, 0.125 mL) in a mixed solvent of ethanol/water (4.625 mL, 0–40 vol% of ethanol) to form Ag(I)-MHA_*p*-MBA complexes, Next, NaOH solution (1 M) was added to the system to adjust the pH to 12. Afterwards, fresh $NaBH_4$ solution (0.1 mL) was added dropwise to reduce the complexes. The bi-thiolate MHA_*p*-MBA-protected Ag_{25} NCs were collected after 2 h for further characterization.

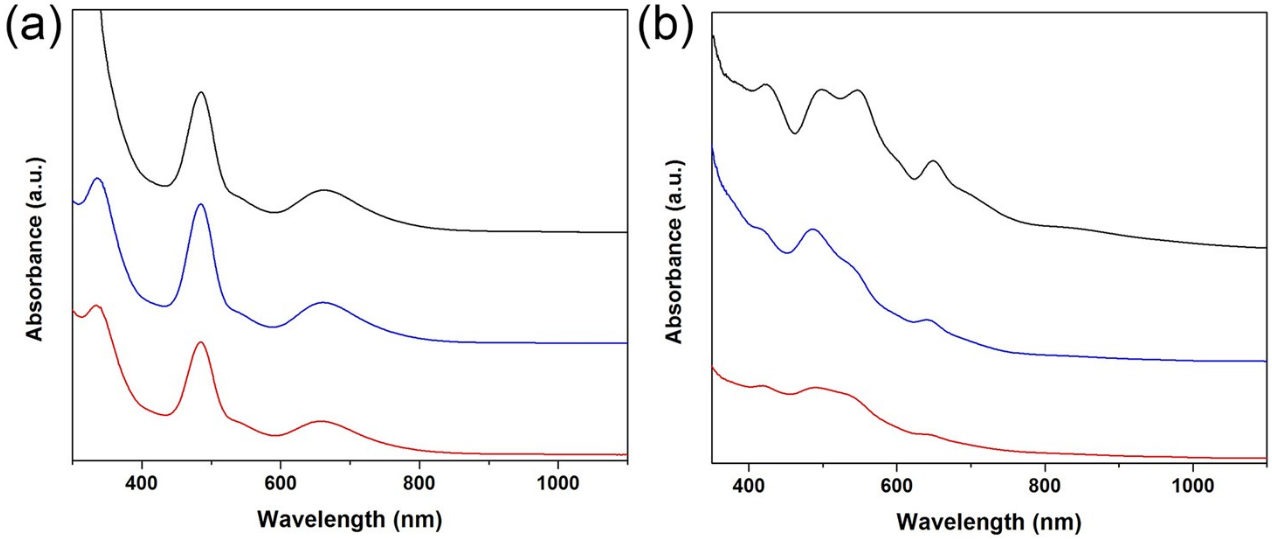

Fig. S1 UV-vis absorption spectra of (a) $Ag_{25}(MHA)_{18}$ NCs and (b) $Ag_{44}(p\text{-}MBA)_{30}$ NCs synthesized at pH 12 in mixed solvents of ethanol/water: 40 vol% ethanol (black curves), 20 vol% ethanol (blue curves) and 0 vol% ethanol (red curves).

Note: As shown in Fig. S1a, the synthesis of $Ag_{25}(MHA)_{18}$ NCs was tolerant with solvent proportions. The absorption features of $Ag_{25}(SR)_{18}$ NCs were observed for the MHA-protected Ag NCs synthesized in 40 vol% ethanol, 20 vol% ethanol, and 0 vol% ethanol, which offers a good opportunity in synthesizing bi-thiolate MHA_*p*-MBA-protected Ag NCs. Similarly, Fig. S1b also showed that $Ag_{44}(p\text{-}MBA)_{30}$ NCs could be synthesized in the same reaction conditions as that for $Ag_{25}(MHA)_{18}$ NCs, although 40 vol% of ethanol was the optimized condition for the synthesis of high-quality *p*-MBA-protected Ag_{44} NCs.

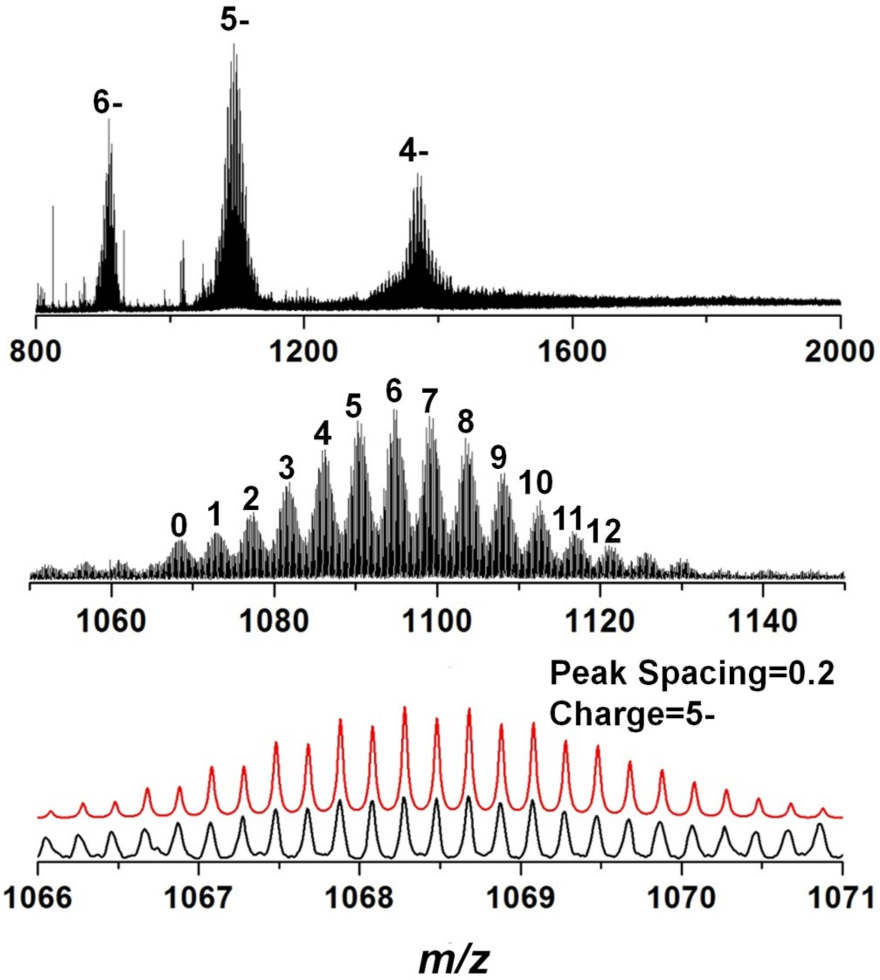

Fig. S2 ESI mass spectra of $Ag_{25}(MHA)_{18}$ NCs. Broad spectrum of $Ag_{25}(MHA)_{18}$ NCs (top panel), zoom-in spectrum of $[Ag_{25}(MHA)_{18} - 4H]^{5-}$ (middle panel), and isotope patterns acquired experimentally (black curve) and theoretically (red curve) of $[Ag_{25}(MHA)_{18} - 4H]^{5-}$ (bottom panel). In the middle panel, peak 0 corresponds to $[Ag_{25}(MHA)_{18} - 4H]^{5-}$, and other peaks (#1–12) are from the successive coordination of [+ Na – H] of peak 0.

Fig. S3 Photograph of native PAGE result of the as-synthesized $Ag_{25}(MHA)_{18}$ NCs.

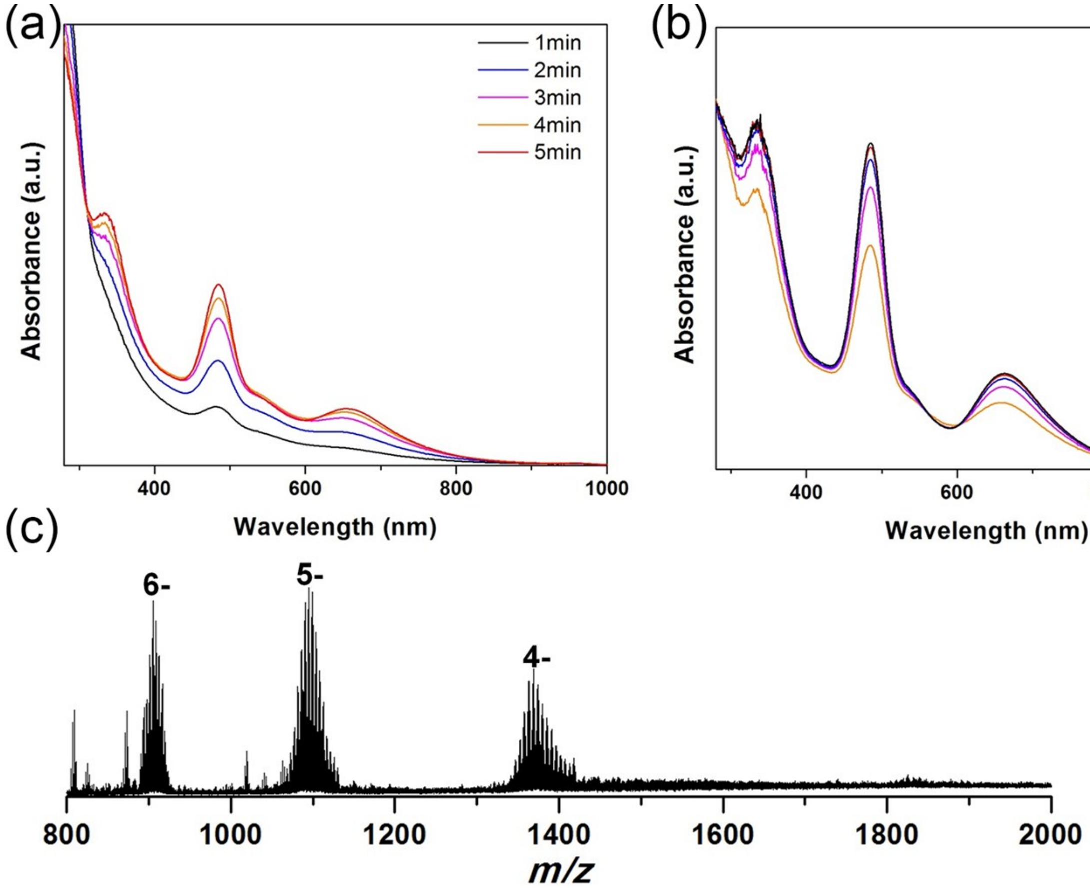

Fig. S4 (a-b) Time evolution UV-vis absorption spectra of the reaction solution during the synthesis of $Ag_{25}(MHA)_{18}$ NCs. (c) ESI mass spectrum of the reaction solution (for the synthesis of $Ag_{25}(MHA)_{18}$ NCs) after 3 min reaction.

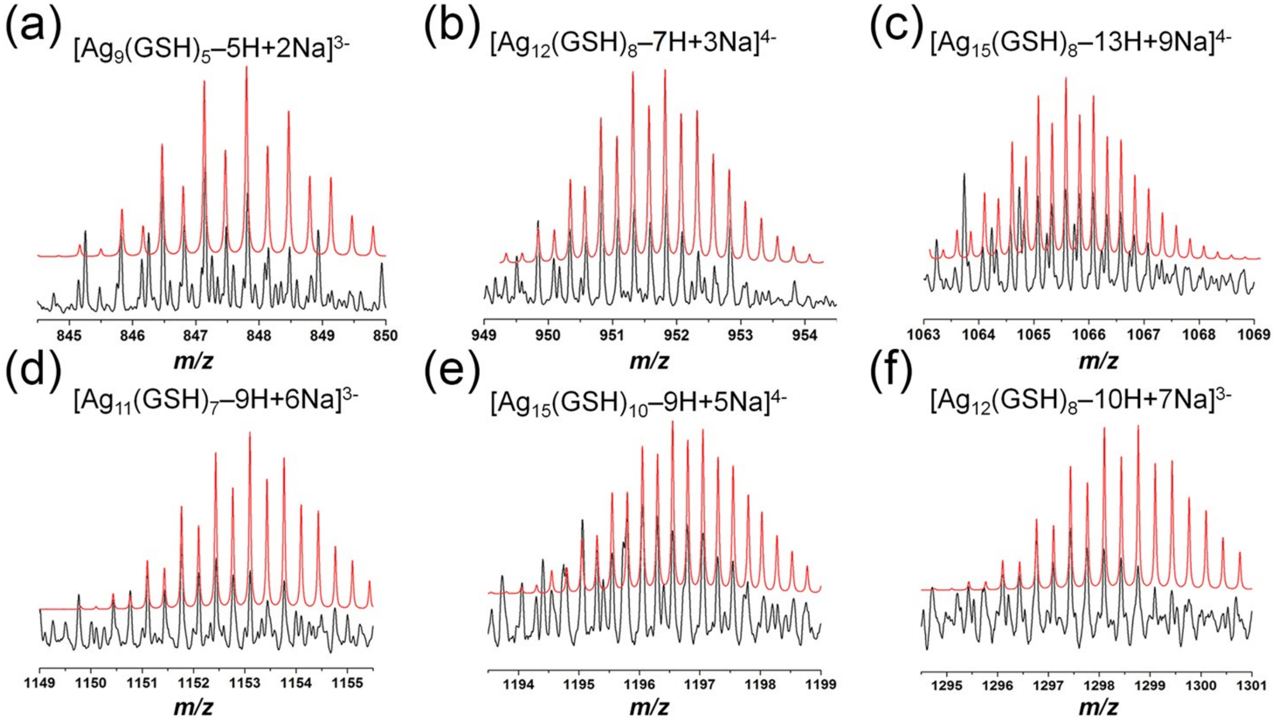

Fig. S5 Detailed ESI mass spectra of the as-synthesized $Ag_{9–15}$ NCs protected by GSH ligand. Isotope patterns acquired experimentally (black curve) and theoretically (red curve) of (a) $[Ag_9(GSH)_5 – 5H + 2Na]^{3-}$, (b) $[Ag_{12}(GSH)_8 – 7H + 3Na]^{4-}$, (c) $[Ag_{15}(GSH)_8 – 13H + 9Na]^{4-}$, (d) $[Ag_{11}(GSH)_7 – 9H + 6Na]^{3-}$, (e) $[Ag_{15}(GSH)_{10} – 9H + 5Na]^{4-}$, and (f) $[Ag_{12}(GSH)_8 – 10H + 7Na]^{3-}$.

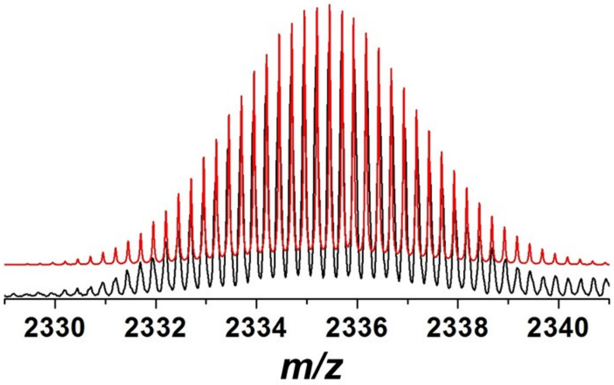

Fig. S6 Isotope patterns of $[Ag_{44}(p\text{-MBA})_{30}]^{4-}$ species acquired experimentally (black curve) and theoretically (red curve).

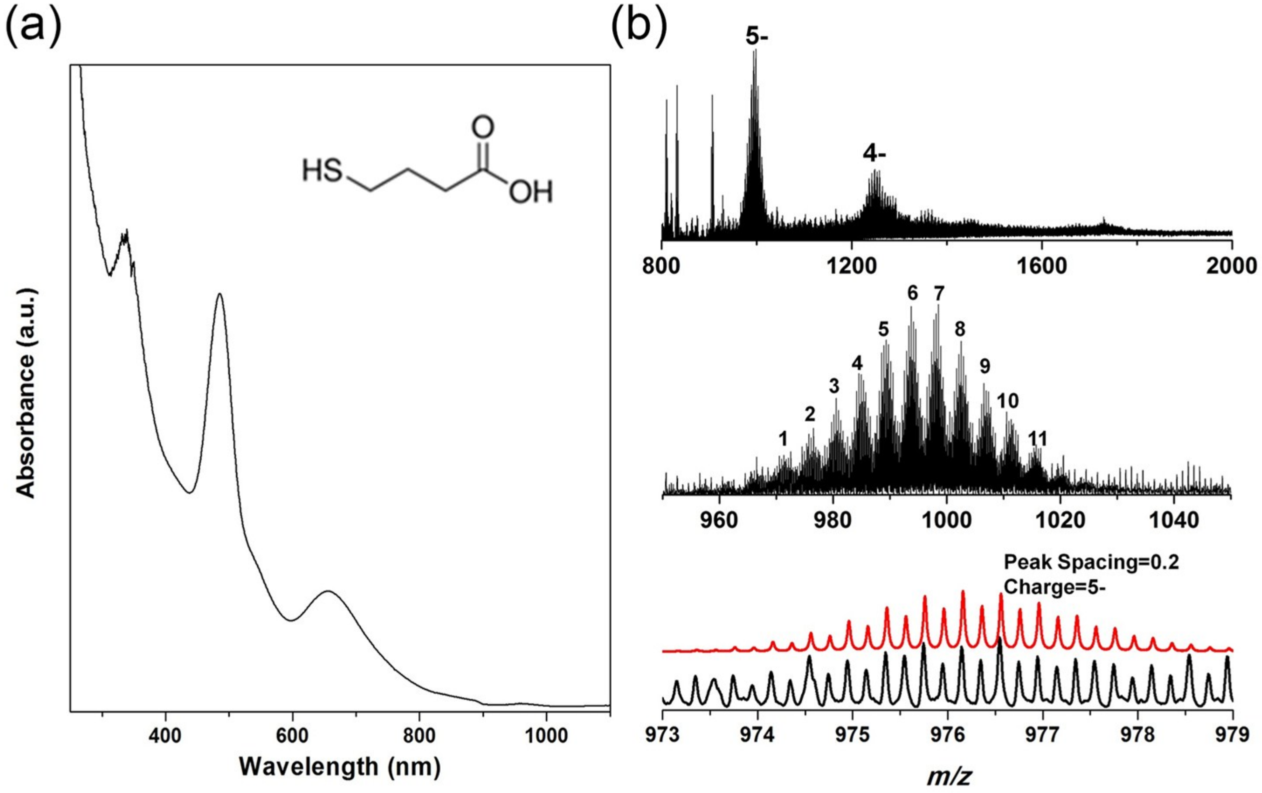

Fig. S7 (a) UV-vis absorption and (b) ESI mass spectra of the as-synthesized $Ag_{25}(MTBA)_{18}$ NCs. The molecular structure of MTBA is shown in the inset of Fig. S7a. In Fig. S7b, a broad spectrum of $Ag_{25}(MTBA)_{18}$ (top panel), zoom-in spectrum of $[Ag_{25}(MTBA)_{18} - 4H]^{5-}$ (middle panel), and isotope patterns of $[Ag_{25}(MTBA)_{18} - 6H + 2Na]^{5-}$ (bottom panel) acquired experimentally (black curve) and theoretically (red curve), were included. In the middle panel, peak 1 corresponds to $[Ag_{25}(MTBA)_{18} - 5H + Na]^{5-}$, and other peaks (#2–11) are from the successive coordination of [+ Na – H] of peak 1.

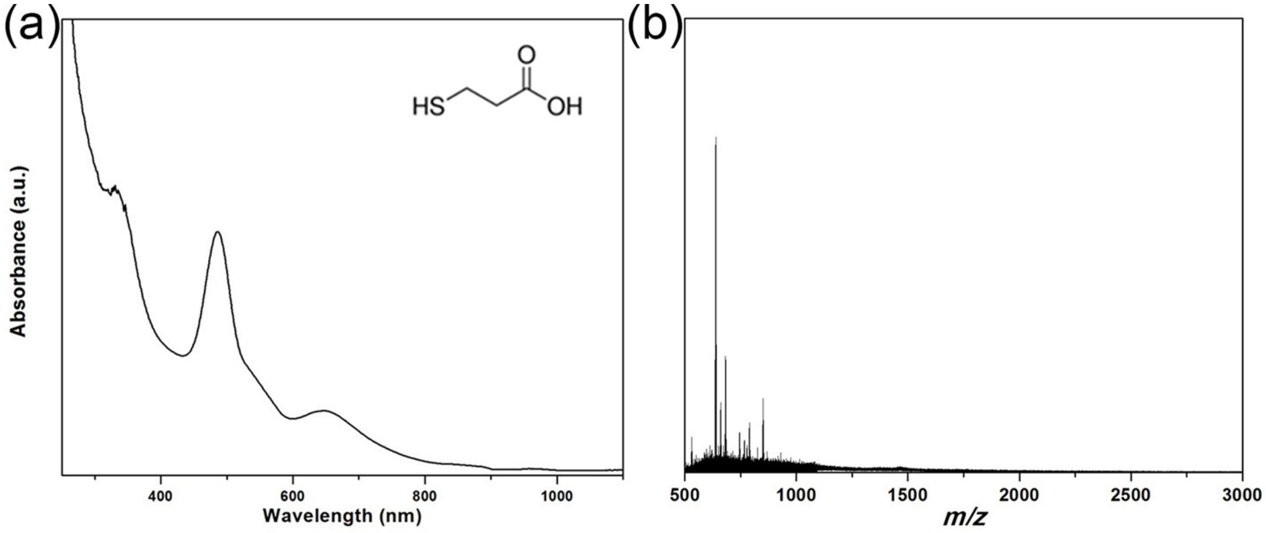

Fig. S8 (a) UV-vis absorption and (b) ESI mass spectrum of the as-synthesized $Ag_{25}(MPA)_{18}$ NCs. The molecular structure of MPA is shown in the inset of Fig. S8a. The well-defined UV-vis absorption feature shown in Fig. S8a confirmed the formation of high-quality $Ag_{25}(MPA)_{18}$ NCs. However, as shown in Fig. S8b, no peak corresponding to $Ag_{25}(MPA)_{18}$ species was observed in the ESI mass spectrum, which suggests that the $Ag_{25}(MPA)_{18}$ NCs were very fragile and could be decomposed during the ionization process of ESI analysis, indicating the poor stability of $Ag_{25}(MPA)_{18}$ NCs.

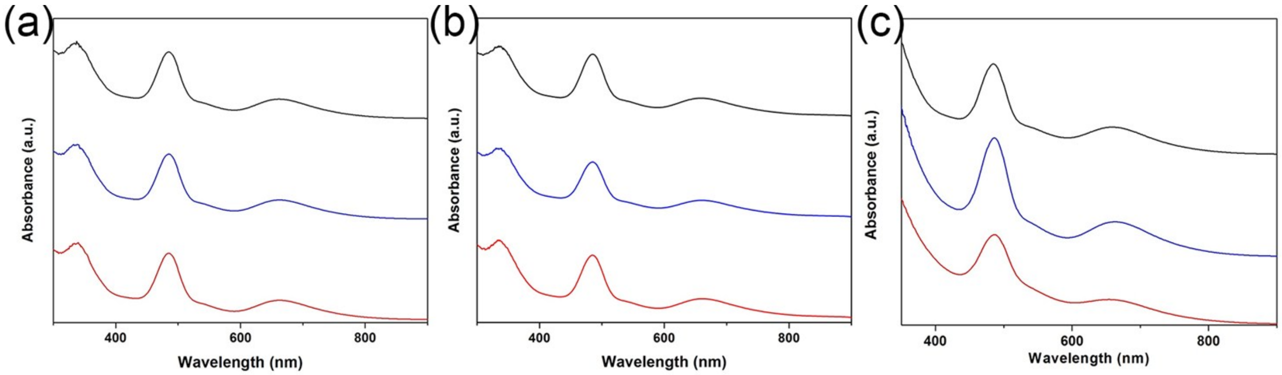

Fig. S9 UV-vis absorption spectra of (a) $Ag_{25}(MHA)_x(MPA)_{18-x}$ NCs, (b) $Ag_{25}(MHA)_x(GSH)_{18-x}$ NCs, and (c) $Ag_{25}(MHA)_x(p\text{-}MBA)_{18-x}$ NCs synthesized with a feeding ratio of MHA-to-MPA (or GSH, or *p*-MBA) of 4:1 (black curves), 2:1 (blue curves) and 1:1 (red curves).

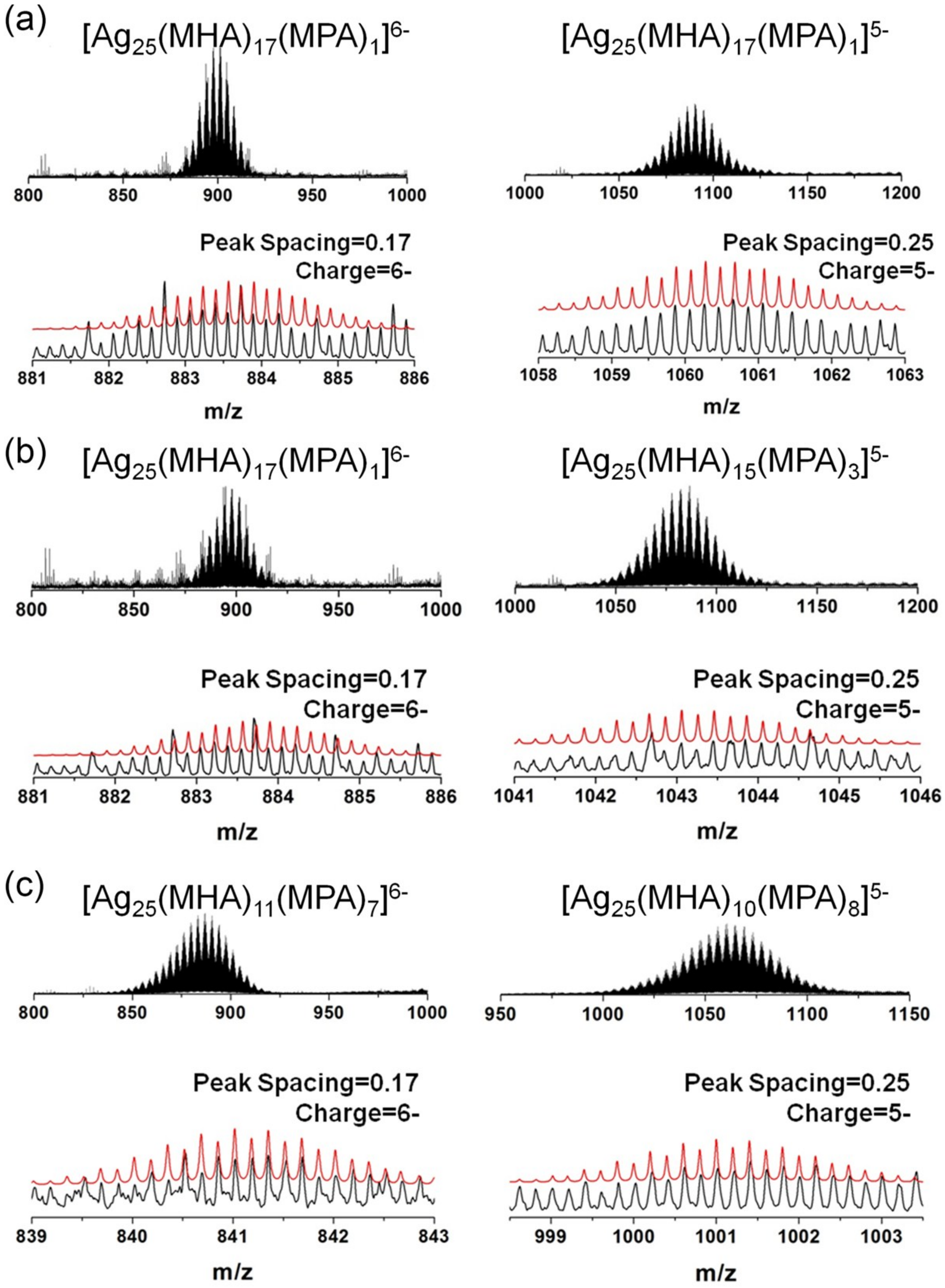

Fig. S10 Zoom-in ESI mass spectra of $Ag_{25}(MHA)_x(MPA)_{18-x}$ NCs (top panels) and corresponding isotope patterns acquired experimentally (black curves) and theoretically (red curves) of $Ag_{25}(MHA)_x(MPA)_{18-x}$ NCs (bottom panels) synthesized with a feeding MHA-to-MPA ratio of (a) 4:1, (b) 2:1, and (c) 1:1.

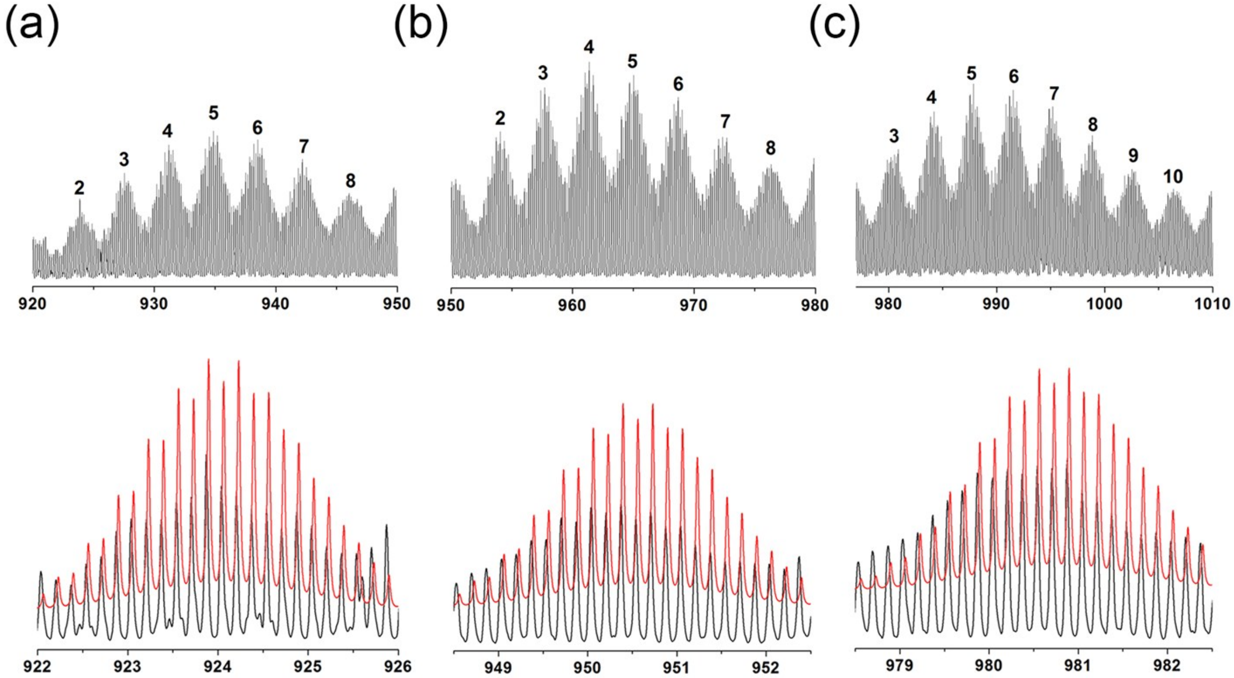

Fig. S11 Zoom-in ESI mass spectra (top panel) and isotope patterns (bottom panel) acquired experimentally (black curves) and theoretically (red curves) of bi-thiolate MHA_GSH-protected Ag_{25} NCs: (a) $[Ag_{25}(MHA)_{17}(GSH) - 7H + 2Na]^{6-}$ species, (b) $[Ag_{25}(MHA)_{16}(GSH)_2 - 7H + 2Na]^{6-}$ species, (c) $[Ag_{25}(MHA)_{15}(GSH)_3 - 8H + 3Na]^{6-}$ species. The peak number labeled in top panels represents the number of [+ Na – H].

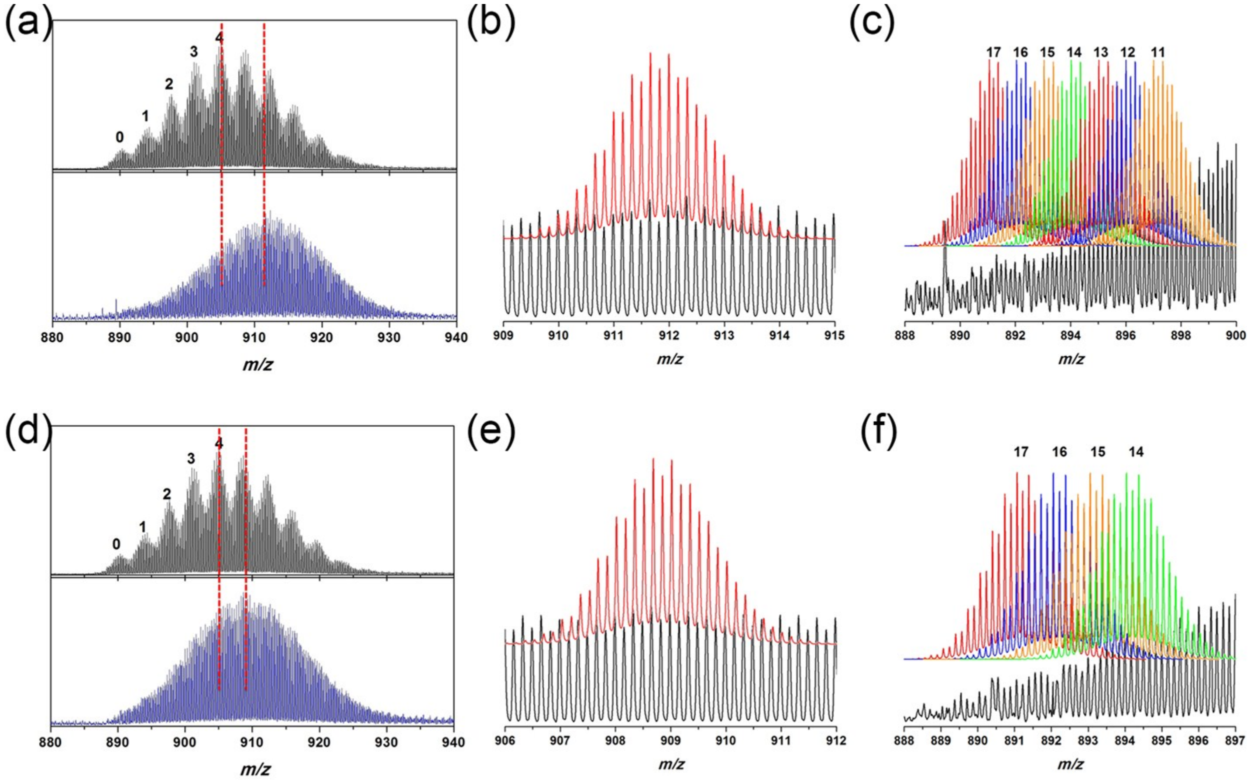

Fig. S12 (a) Zoom-in ESI mass spectra (the peak number represents the number of [+ Na – H]) of $Ag_{25}(MHA)_{18}$ (top panel) and $Ag_{25}(MHA)_x(p\text{-}MBA)_{18-x}$ (bottom panel, with a feeding MHA-to-*p*-MBA ratio of 2:1). The dotted red lines marked the right shift from $[Ag_{25}(MHA)_{18} - 9H + 4Na]^{6-}$ to $[Ag_{25}(MHA)_{11}(p\text{-}MBA)_7 - 9H + 4Na]^{6-}$. (b) Isotope patterns acquired experimentally (black curves) and theoretically (red curves) of $[Ag_{25}(MHA)_{11}(p\text{-}MBA)_7 - 9H + 4Na]^{6-}$. (c) Isotope patterns acquired experimentally (black curves) and theoretically (color curves) of $[Ag_{25}(MHA)_{11-17}(p\text{-}MBA)_{7-1} - 5H]^6$ (the number labeled in the spectra shows the number of MHA). (d) Zoom-in ESI mass spectra (the peak number represents the number of [+ Na – H]) of $Ag_{25}(MHA)_{18}$ (top panel) and $Ag_{25}(MHA)_x(p\text{-}MBA)_{18-x}$ (bottom panel, feeding ratio of MHA-to-*p*-MBA is 1:1). The dotted red lines marked the right shift from $[Ag_{25}(MHA)_{18} - 9H + 4Na]^{6-}$ to $[Ag_{25}(MHA)_{14}(p\text{-}MBA)_4 - 9H + 4Na]^{6-}$. (e) Isotope patterns acquired experimentally (black curves) and theoretically (red curves) of $[Ag_{25}(MHA)_{14}(p\text{-}MBA)_4 - 9H + 4Na]^{6-}$. (f) Isotope patterns acquired experimentally (black curves) and theoretically (color curves) of $[Ag_{25}(MHA)_{14-17}(p\text{-}MBA)_{4-1} - 5H]^6$ (the number labeled in the spectra shows the number of MHA).

Notes: The slight difference between MHA and *p*-MBA in molecular weights leads to the peak overlaps in the ESI mass spectrum of $Ag_{25}(MHA)_x(p\text{-}MBA)_{18-x}$ NCs, thereby it is difficult to identify the exact formula of the species of $Ag_{25}(MHA)_x(p\text{-}MBA)_{18-x}$ NCs. To determine the maximum number of *p*-MBA in $Ag_{25}(MHA)_x(p\text{-}MBA)_{18-x}$ NCs, the shift of the highest peak of $Ag_{25}(MHA)_{18}$ NCs (i.e., $[Ag_{25}(MHA)_{18} - 9H + 4Na]^{6-}$) to that of $Ag_{25}(MHA)_x(p\text{-}MBA)_{18-x}$ NCs was compared. Based on the difference of the *m/z* values of the highest peaks, the formula $[Ag_{25}(MHA)_x(p\text{-}MBA)_{18-x}]^{6-}$ was determined accordingly.

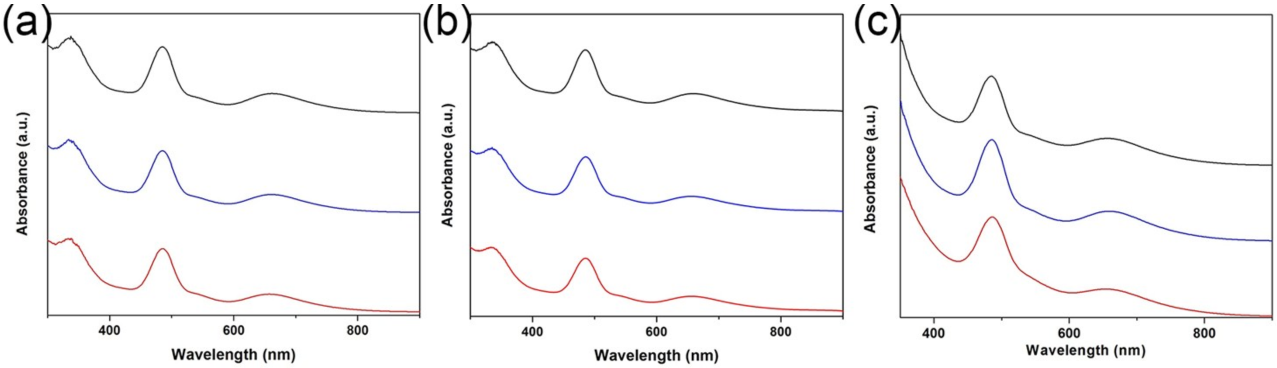

Fig. S13 UV-vis absorption spectra of (a) $Ag_{25}(MHA)_x(MPA)_{18-x}$ NCs and (b) $Ag_{25}(MHA)_x(GSH)_{18-x}$ NCs (feeding MHA-to-MPA or -GSH ratio of 1:1) after reaction of 10 min (black curves), 20 min (blue curves) and 30 min (red curves). (c) UV-vis absorption spectra of $Ag_{25}(MHA)_x(p\text{-}MBA)_{18-x}$ NCs (feeding MHA-to-*p*-MBA ratio of 1:1) after reaction of 1 h (black curves), 1.5 h (blue curves) and 2 h (red curves).

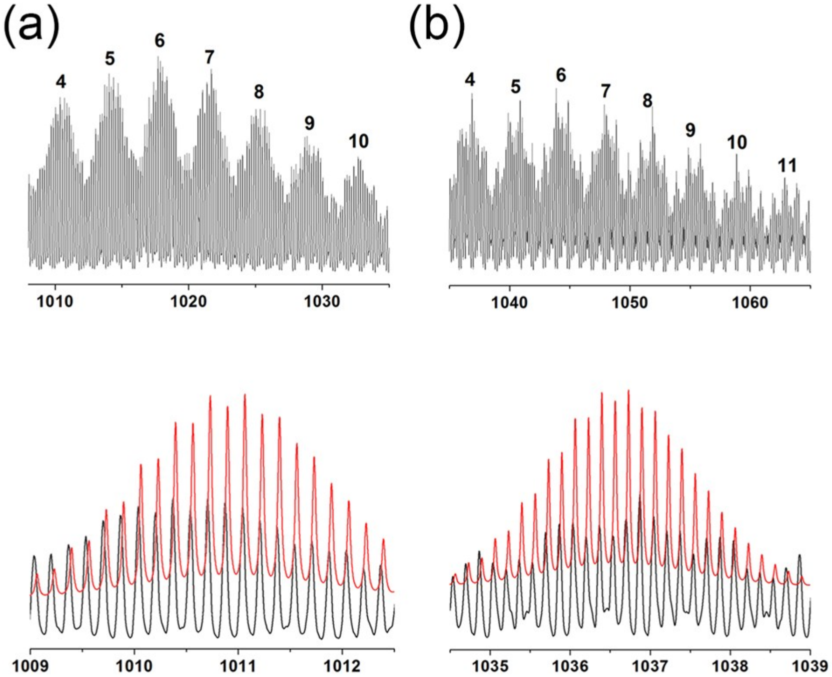

Fig. S14 Zoom-in ESI mass spectra (top panel) and isotope patterns (bottom panel) acquired experimentally (black curves) and theoretically (red curves) of bi-thiolate MHA_GSH-protected Ag_{25} NCs: (a) $[Ag_{25}(MHA)_{14}(GSH)_4 - 9H + 4Na]^{6-}$ species, (b) $[Ag_{25}(MHA)_{13}(GSH)_5 - 9H + 4Na]^{6-}$ species. The peak number labeled in top panels represents the number of [+ Na – H].

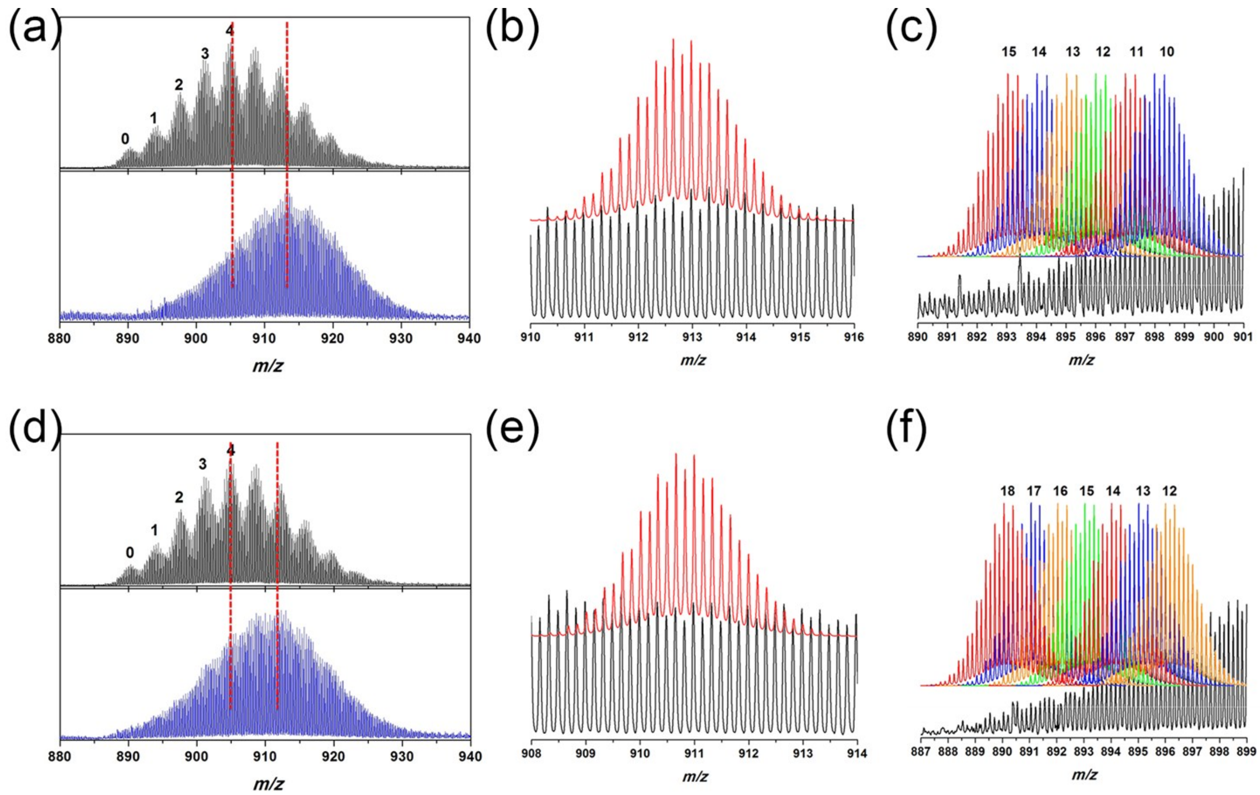

Fig. S15 (a) Zoom-in ESI mass spectra (the peak number represents the number of [+ Na – H]) of $Ag_{25}(MHA)_{18}$ (top panel) and $Ag_{25}(MHA)_x(p\text{-}MBA)_{18-x}$ (bottom panel, feeding MHA-to-*p*-MBA ratio is 1:1 and the reaction time is 1 h). The dotted red lines marked the red shift from $[Ag_{25}(MHA)_{18} - 9H + 4Na]^{6-}$ to $[Ag_{25}(MHA)_{10}(p\text{-}MBA)_8 - 9H + 4Na]^{6-}$. (b) Isotope patterns acquired experimentally (black curves) and theoretically (red curves) of $[Ag_{25}(MHA)_{10}(p\text{-}MBA)_8 - 9H + 4Na]^{6-}$. (c) Isotope patterns acquired experimentally (black curves) and theoretically (color curves) of $[Ag_{25}(MHA)_{10–15}(p\text{-}MBA)_{8–3} - 5H]^{6}$ (the number shown in the spectra represents the number of MHA). (d) Zoom-in ESI mass spectra (the peak number represents the number of [+ Na – H]) of $Ag_{25}(MHA)_{18}$ (top panel) and $Ag_{25}(MHA)_x(p\text{-}MBA)_{18-x}$ (bottom panel, feeding MHA-to-*p*-MBA ratio is 1:1 and the reaction time is 1.5 h). The dotted red lines marked the red shift from $[Ag_{25}(MHA)_{18} - 9H + 4Na]^{6-}$ to $[Ag_{25}(MHA)_{12}(p\text{-}MBA)_6 - 9H + 4Na]^{6-}$. (e) Isotope patterns acquired experimentally (black curves) and theoretically (red curves) of $[Ag_{25}(MHA)_{12}(p\text{-}MBA)_6 - 9H + 4Na]^{6-}$. (f) Isotope patterns acquired experimentally (black curves) and theoretically (color curves) of $[Ag_{25}(MHA)_{12–18}(p\text{-}MBA)_{6–0} - 5H]^{6}$ (the number shown in the spectra represents the number of MHA).